Inorganic Chemistry
Article

Inorg. Chem. **2011**, *50*, 1089–1097 **1089**
DOI: 10.1021/ic101914e

Crystal Chemistry and Stability of "$Li_7La_3Zr_2O_{12}$" Garnet: A Fast Lithium-Ion Conductor

Charles A. Geiger,*,† Evgeny Alekseev,† Biljana Lazic,‡ Martin Fisch,‡ Thomas Armbruster,‡ Ramona Langner,§ Michael Fechtelkord,§ Namjun Kim,# Thomas Pettke,‡ and Werner Weppner||

†*Institut für Geowissenschaften, Abteilung Mineralogie, Christian-Albrechts-Universität zu Kiel, D-24118 Kiel, Germany,* ‡*Mineralogische Kristallographie, Institut für Geologie, Universität Bern, CH-3012 Bern, Switzerland,* §*Institut für Geologie, Mineralogie und Geophysik, Ruhr-Universität Bochum, D-44780 Bochum, Germany,* #*Department of Geological and Environmental Sciences, Stanford University, Stanford, California 94305-2115, United States , and* ||*Institut für Anorganische Chemie, Christian-Albrechts-Universität zu Kiel, Otto-Hahn-Platz 6-7, D-24118 Kiel, Germany*

Received September 18, 2010

Recent research has shown that certain Li-oxide garnets with high mechanical, thermal, chemical, and electrochemical stability are excellent fast Li-ion conductors. However, the detailed crystal chemistry of Li-oxide garnets is not well understood, nor is the relationship between crystal chemistry and conduction behavior. An investigation was undertaken to understand the crystal chemical and structural properties, as well as the stability relations, of $Li_7La_3Zr_2O_{12}$ garnet, which is the best conducting Li-oxide garnet discovered to date. Two different sintering methods produced Li-oxide garnet but with slightly different compositions and different grain sizes. The first sintering method, involving ceramic crucibles in initial synthesis steps and later sealed Pt capsules, produced single crystals up to roughly 100 μm in size. Electron microprobe and laser ablation inductively coupled plasma mass spectrometry (ICP-MS) measurements show small amounts of Al in the garnet, probably originating from the crucibles. The crystal structure of this phase was determined using X-ray single-crystal diffraction every 100 K from 100 K up to 500 K. The crystals are cubic with space group $Ia\bar{3}d$ at all temperatures. The atomic displacement parameters and Li-site occupancies were measured. Li atoms could be located on at least two structural sites that are partially occupied, while other Li atoms in the structure appear to be delocalized. ^{27}Al NMR spectra show two main resonances that are interpreted as indicating that minor Al occurs on the two different Li sites. Li NMR spectra show a single narrow resonance at 1.2−1.3 ppm indicating fast Li-ion diffusion at room temperature. The chemical shift value indicates that the Li atoms spend most of their time at the tetrahedrally coordinated C (24*d*) site. The second synthesis method, using solely Pt crucibles during sintering, produced fine-grained $Li_7La_3Zr_2O_{12}$ crystals. This material was studied by X-ray powder diffraction at different temperatures between 25 and 200 °C. This phase is tetragonal at room temperature and undergoes a phase transition to a cubic phase between 100 and 150 °C. Cubic "$Li_7La_3Zr_2O_{12}$" may be stabilized at ambient conditions relative to its slightly less conducting tetragonal modification via small amounts of Al^{3+}. Several crystal chemical properties appear to promote the high Li-ion conductivity in cubic Al-containing $Li_7La_3Zr_2O_{12}$. They are (i) isotropic three-dimensional Li-diffusion pathways, (ii) closely spaced Li sites and Li delocalization that allow for easy and fast Li diffusion, and (iii) low occupancies at the Li sites, which may also be enhanced by the heterovalent substitution $Al^{3+} \leftrightarrow 3Li$.

Introduction

Rechargeable Li-ion batteries are essential power sources for a large variety of portable electronic devices. Moreover, because the next generation of electric cars will also use Li-ion cells, fast Li-ion conductors are crucial in today's industry and for societal needs. Most Li-ion batteries now in use have liquid and polymer-supported electrolytes, and they can have a number of unwanted, if not dangerous, properties such as dendrite formation, leakage, and flammability. Thus, there is great current interest in finding and developing new solid-state fast Li-ion conductors that are thermally and chemically stable and that have high energy densities. Recent research along these lines has shown that certain Li-oxide garnets have the necessary high-ionic conductivities, as well as good chemical

*Corresponding author. Present address: Fachbereich Materialforschung und Physik, Abteilung Mineralogie, Universität Salzburg, Hellbrunnerstrasse 34, A-5020 Salzburg, Austria. Fax (0662) 8044-5407. Tel. (0662) 8044-5407. E-mail: ca.geiger@sbg.ac.at.

(1) Thangadurai, V.; Kaack, H; Weppner, W. *J. Am. Ceram. Soc.* **2003**, *86*, 437–440.

Published on Web 12/28/2010

and physical properties, to be considered as potential electrolytes in solid-state batteries.[1−8]

There have been a number of diffraction studies, using both X-rays and neutrons, to determine the crystal structures of a wide variety of Li-oxide garnets.[9−23] Much has been learned, but considerable confusion and uncertainties still exist in terms of their exact crystal chemical properties. Neither the nature behind the ion-conduction process nor the relationship between garnet chemistry and conduction behavior is well understood. Li-oxide garnets pose problems in diffraction experiments. X-ray powder-based structure determinations are plagued by the problem of poor scattering by Li, while neutron powder diffraction measurements are more sensitive at detecting the Li atom, but the data sets are still limited. Both methods have problems in determining atomic displacement parameters (adps) correctly. The issue is important because a quantitative determination of Li-site occupancy, which is necessary to understand the diffusion behavior, depends on a correct measurement of the adps. Up to now, there are few single-crystal diffraction determinations with large data sets on Li-oxide garnets,[20,21] and they also can be plagued with problems associated with describing the Li atoms correctly.

Research has shown that a number of Li-oxide garnet compositions that have more than three Li cations in the formula unit are excellent ion conductors, as recently reviewed.[8] Work has shown that cubic garnet of nominal composition $Li_7La_3Zr_2O_{12}$ has some of the highest measured ion conductivities for the Li-oxide class of garnets,[5] comparable to or even greater than those measured on other well-known fast Li-ion conductors such as Li_3N, Li-β-Al_2O_3, or LIPON. Moreover, it has excellent physical and chemical properties that are needed for use in solid-state batteries. However, the crystal structure of cubic "$Li_7La_3Zr_2O_{12}$" (we give the composition in quotes because the exact composition was not reported) has not been solved, nor is the reason for its high ionic conductivity understood. Initial work on this phase focused primarily on its stability and conduction behavior.[5] Structural characterization was rudimentary and was done using simple X-ray powder diffraction, and a comparison of its diffraction pattern to $Li_5La_3Nb_2O_{12}$ garnet indicated that it was cubic.

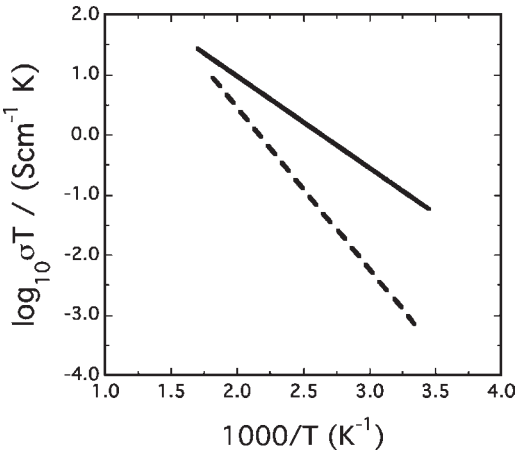

Figure 1. Arrhenius plot for the total (bulk + grain boundary) lithium-ion conductivity of "$Li_7La_3Zr_2O_{12}$". Conductivity for the cubic phase is shown by the solid line and by the dashed line for the tetragonal phase.

The crystal structure of tetragonal $Li_7La_3Zr_2O_{12}$ garnet was recently investigated using neutron powder and X-ray single-crystal methods, and its composition and conductivity behavior were also studied.[20] It has space group symmetry $I4_1/acd$ and it is characterized by lower ion conductivity compared to the cubic phase (Figure 1). The reason(s) for the occurrence of different $Li_7La_3Zr_2O_{12}$ structures at ambient conditions and for differences in their ion conductivity behavior are not understood.

In order to optimize ion-conduction properties and also to understand fully the physical nature behind the conduction process in the Li-oxide garnet class of phases, it is necessary to know their crystal chemical properties in detail. This study was initiated by the need to determine the crystal chemical properties of "$Li_7La_3Zr_2O_{12}$" garnet and to investigate the reasons behind its high ion conductivity. An emphasis was made on obtaining single crystals of large enough size so that a high quality X-ray single-crystal diffraction data set could be obtained. Electron microprobe and laser ablation ICP-MS measurements were undertaken to determine the precise composition and to check for zoning and the presence of impurity phases. In addition, ^{27}Al MAS and MQMAS NMR spectroscopic determinations at different field strengths, as well as $^{6/7}$Li MAS measurements, were made to characterize the local structural environment and to obtain dynamic information on the Li atoms. Finally, X-ray power diffraction measurements were made between 25 and 200 °C to study phase stability.

Experimental Methods

Synthesis. Single-crystal synthesis can be done using a variety of methods. We undertook solid-state sintering, flux-based (i.e., molten Li-borates) and hydrothermal experiments at elevated pressures in order to try to obtain $Li_7La_3Zr_2O_{12}$ single crystals. After much study, we concentrated our efforts on 1-atm sintering methods generally similar to those used in refs 5 and 20.

(2) Thangadurai, V.; Weppner, W. *J. Am. Ceram. Soc.* **2005**, *88*, 411–418.
(3) Thangadurai, V.; Weppner, W. *Adv. Funct. Mater.* **2005**, *15*, 107–112.
(4) Thangadurai, V.; Weppner, W. *J. Solid State Chem.* **2006**, *179*, 974–984.
(5) Murugan, R.; Thangadurai, V.; Weppner, W. *Angew. Chem.* **2007**, *119*, 7925–7928.
(6) Murugan, R.; Weppner, W.; Schmid-Beurmann, P.; Thangadurai, V. *Mater. Sci. Eng.* **2007**, *143*, 14–20.
(7) Murugan, R.; Weppner, W.; Schmid-Beurmann, P.; Thangadurai, V. *Mater. Res. Bull.* **2008**, *43*, 2579–2591.
(8) Ramzy, A.; Thangadurai, V. *ACS Appl. Mater. Interfaces* **2010**, *2*, 385–390.
(9) Hyooma, H.; Hayashi, K: *Mater. Res. Bull.* **1988**, *23*, 1399–1407.
(10) Mazza, D. *Mater. Lett.* **1988**, *7*, 205–207.
(11) Cussen, E. J. *Chem. Commun.* **2006**, 412–413.
(12) O'Callaghan, M. P.; Lynham, D. R.; Cussen, E. J.; Chen, G. Z. *Chem. Mater.* **2006**, *18*, 4681–4189.
(13) Cussen, E. J.; Yip, T. W. S. *J. Solid State Chem.* **2007**, *180*, 1832–1839.
(14) O'Callaghan, M. P.; Cussen, E. J. *Chem. Commun.* **2007**, *10*, 2048–2050.
(15) Percival, J.; Kendrick, E.; Slater, P. R. *Mater. Res. Bull.* **2008**, *43*, 765–770.
(16) O'Callaghan, M. P.; Cussen, E. J. *Solid State Sci.* **2008**, *10*, 390–395.
(17) Percival, J.; Kendrick, E.; Slater, P. R. *Solid State Ionics* **2008**, *179*, 1666–1669.
(18) Percival, J.; Kendrick, E.; Smith, R. I.; Slater, P. R. *Dalton Trans.* **2009**, 5177–5181.
(19) O'Callaghan, M. P.; Powell, A. S.; Titman, J. J.; Chen, G. Z.; Cussen, E. J. *Chem. Mater.* **2008**, *20*, 2360–2369.
(20) Awaka, J.; Kijima, N.; Hayakawa, H.; Akimoto, J. *J. Solid State Chem.* **2009**, *182*, 2046–2052.
(21) Roof, I. P.; Smith, M. D.; Cussen, E. J.; zur Loye, H.-C. *J. Solid State Chem.* **2009**, *182*, 295–300.
(22) Yoo, C.-Y.; Kim, S.-C.; Lee, S.-S.; Kim, S.-J. *Acta Crystallogr.* **2009**, *E65*, 74.
(23) Awaka, J.; Kijima, N.; Kataoka, K.; Hayakawa, H.; Oshima, K.; Akimoto, J. *J. Solid State Chem.* **2010**, *183*, 180–185.

In the first method, synthesis experiments were made using mixtures of oxides and carbonates, namely, ZrO_2 (99% Aldrich), La_2O_3 (99.99% Chempur), and Li_2CO_3 (99% Alfa). ZrO_2 and La_2O_3 were first heated at about 1273 K and Li_2CO_3 at 573 K in ceramic-based crucibles. The components were then finely mixed in stoichiometric proportions to give $Li_7La_3Zr_2O_{12}$ with 5 wt % extra Li_2CO_3 and were pressed to pellets and sintered at 1073 K. The reaction product was ground and seeded with small amounts of fine-grained $Li_7La_3Zr_2O_{12}$ that had been made from previous sintering experiments. Dense pressed pellets were then welded into Pt(Pd)- and/or Au-capsules about 2 cm long and 5 mm diameter. The capsules were heated at different rates (50−300 °C/h) and held at temperatures of 1173−1373 K overnight in a box furnace. The resulting hard and brittle pellet used for further study was light tan in color and polycrystalline. The X-ray powder pattern is similar to that observed in ref 5 and contains an additional few weak reflections that could not be indexed to garnet. Upon observation with a binocular scope, a distribution of relatively equidimensional crystals with a garnet-like habit could be observed in the pellet. The largest ranged up to roughly 100 μm in size. A number of crystals were separated from the pellet and investigated by X-ray methods to see if they were single crystal in nature. Several were found and used for detailed X-ray study.

Polycrystalline $Li_7La_3Zr_2O_{12}$ was also synthesized using solid-state reaction techniques following exactly those described in ref 20. In this case, we note that sintering was done solely in a Pt crucible.

Compositional Characterization. A small polycrystalline chip from the first synthesis method, using a ceramic crucible and a Pt capsule, was embedded in an epoxy holder and the surface was ground and then polished using diamond paste. The composition of several single crystals was investigated using a JEOL JXA-8900R electron-probe microanalyzer. The crystals could be observed in the microprobe from the grain boundary relationships. Backscattered electron maps were also made to check for the presence of additional phases. The general composition and the presence of all common elements were first checked using energy dispersive spectroscopy (EDS) analysis. Al, La, and Zr were detected. Li is too light to be measured. Next, quantitative wavelength dispersive spectroscopy (WDS) analyses were made for the former three elements using an accelerating voltage of 20 kV and a beam current of 40 nA, with a beam diameter of 1 μm. A number of analyses were made on various points on four different single crystals of about 50−100 μm in diameter in the polycrystalline aggregate. The following mineral and phase standards were used: corundum (Al), zircon (Zr), and $LaPO_4$ (La). The PRZ method (modified ZAF) was used for data correction.

Laser ablation inductively coupled plasma mass spectrometry (LA-ICP-MS) measurements were performed on the same chip at the University of Bern using a GeoLasPro ArF excimer laser system combined with an Elan DRCe quadrupole ICP-MS, employing analytical and ICP-MS optimization strategies reported elsewhere.[24] The dual detector of the instrument was calibrated prior to analysis for all analytes recorded (^{7}Li, ^{27}Al, ^{90}Zr, and ^{139}La). The SRM 610 glass from NIST was used to calibrate analyte sensitivities (Li = 485 μg g^{-1}, Al = 10790 μg g^{-1}, Zr = 437 μg g^{-1}, La = 440 μg g^{-1}), and summation of the element oxides to 100 wt % was used for internal standardization. Data were reduced using the SILLS program.[25] Because LA-ICP-MS always analyzes a volume (here a cylinder of 24 μm diameter and < 20 μm height), compositional inhomogeneity with depth can be recorded. Each transient signal was thus revisited for signal interval selection to avoid any Al contribution not coming from the garnet (see below). To explore for potential fractionation effects relating to plasma aerosol load,[26] tests were performed with laser beam sizes ranging from 16 to 44 μm. No problems were observed except when 16 μm sample analyses were calibrated with 44 μm standard shots. Analyses where thus performed by approximately matching the aerosol load of the plasma between standard and unknown.

^{27}Al MAS and MQMAS NMR and ^{7}Li MAS and ^{6}Li MAS NMR Spectroscopy. Solid-state NMR spectra were recorded on the first garnet synthesis product (i.e., that containing Al) using a Bruker ASX 400 spectrometer at Bochum University and a Varian Unity/Inova 600 spectrometer at Stanford University. All measurements were made at room temperature on the same sample that was characterized by X-ray powder diffraction.

At Bochum the ^{27}Al MAS and MQMAS NMR measurements were carried out at 104.27 MHz using a standard Bruker 4 mm MAS probe with sample spinning at 12.5 kHz. An aqueous solution of $AlCl_3$ was used for the reference standard. For the ^{27}Al MAS NMR experiments, a short single pulse duration of 0.6 μs was used to ensure homogeneous excitation of the central and all satellite transitions. A recycle delay of 100 ms was used, and 50 000 scans were accumulated. For the multiple-quantum magic-angle spinning (MQMAS) NMR experiments[27] a t_1-increment of 20 μs and a recycle delay of 2 s were used. The duration of the first pulse was 2.1 μs and that of the second pulse 1.1 s. (The 90 degree pulse time for aqueous $AlCl_3$-solution was 1.4 μs.) 900 scans were accumulated. A total of 128 t_1-increments were achieved.

At Stanford, a 3.2 mm Varian T3MAS probe was used and single-pulse experiments were carried out with a radio frequency pulse length of 0.23 μs (which corresponds to $\pi/18$ for the aqueous reference of 0.1 M $Al(NO_3)_3$ solution at 0 ppm) at spinning speeds of 20 kHz. Quadrupolar line shapes were simulated using the STARS software package (Varian).

^{7}Li MAS and ^{6}Li MAS NMR spectra were recorded at transmitter frequencies of 155.5 and 58.9 MHz, respectively, at Bochum University. A 1 M aqueous solution of LiCl was used as the standard and a Bruker 4 mm MAS probe was used at a rotation frequency of 12.5 kHz. For the ^{7}Li MAS NMR experiment a single-pulse duration of 0.6 μs and a recycle delay of 100 μs were adopted, and 10,000 scans were accumulated. In the ^{6}Li MAS NMR experiment the single-pulse duration was 3 μs, the recycle delay was 10 and 500 scans were accumulated.

X-ray Single-Crystal-Structure Determination and Powder Diffraction. A single crystal about 60 μm in diameter was separated from the polycrystalline pellet of the Al-containing "$Li_7La_3Zr_2O_{12}$". It was mounted on a glass fiber and studied with a Bruker SMART APEX II CCD diffractometer. Data collection was done every 100 K starting at 100 K up to 500 K. At room temperature a total of 16 079 reflections, defining space-group $Ia\bar{3}d$, were collected up to θ = 45.32° using monochromatic MoKα radiation (λ = 0.71073 Å). A unit-cell dimension of a = 12.97510(10) (a = 12.9682(6)[5]) was refined using least-squares techniques. The data were corrected for Lorentz polarization, absorption, and background effects. Additional information pertinent to the data collection is given in Table 1. The SHELXL 97 program was used for the determination and refinement of the structure. The treatment for absorption was found to be significant in a determination of the Li sites in the structure.

X-ray powder diffraction measurements on the $Li_7La_3Zr_2O_{12}$ material synthesized in a Pt crucible following ref 20 were made with a PANalytical X'Pert PRO MPD diffractometer. It is equipped with an Anton-Paar HTK1200 high temperature goniometer

(24) Pettke, T. Laser Ablation ICP-MS in the Earth Sciences: Current Practices and Outstanding Issues. *Mineralogical Association of Canada Short Course Series*; Sylvester, P., Ed.; Mineralogical Association of Canada: Québec, Canada, **2008**; Vol. *40*, pp 189−218.

(25) Guillong, M.; Meier, D. L.; Allan, M. M.; Heinrich, C. A.; Yardley, B. W. D. Laser Ablation ICP-MS in the Earth Sciences: Current Practices and Outstanding Issues. *Mineralogical Association of Canada Short Course Series*; Sylvester, P., Ed.; Mineralogical Association of Canada: Québec, Canada, **2008**; Vol. *40*, pp 328−333.

(26) Kroslakova, I.; Gunther, D. *J. Anal. Atom. Spect.* **2007**, *22*, 51–62.

(27) Medek, A; Harwood, J. S.; Frydman, L. *J. Am. Chem. Soc.* **1995**, *117*, 12779–12787.

Table 1. Crystallographic Data and Refinement Parameters for Cubic Al-Containing $Li_7La_3Zr_2O_{12}$

a (Å)	12.9751(1)
V (Å^3)	2184.40(3)
space group	$Ia\bar{3}d$
F_{000}	2944
μ (cm^{-1})	13.384
Z	8
D_{calc} (g/cm^3)	5.107
radiation	MoKα
absorption correction	multiscan
R_{int}	0.0341
total ref	16079
unique ref	772
unique ref $\lvert F_0\rvert \geq 4\sigma_F$	638
R_1	0.028
wR_2	0.0511
S	1.211

Table 2. Chemical Analysis on Cubic Al-Containing $Li_7La_3Zr_2O_{12}$[a]

	microprobe (wt %)	LA-ICP-MS[c] (wt %)
La_2O_3	56.86 (0.8)	60.3 (0.4)
ZrO_2	28.89 (0.5)	27.3 (0.3)
Al_2O_3	1.36 (0.2)	1.16 (0.23)
Li_2O	12.50[b]	11.2 (0.4)
total	99.61	100.0[c]

[a] Values in brackets are 1 standard deviation of 10 analyses. [b] Theoretical amount of $Li_7La_3Zr_2O_{12}$. [c] Data were normalized to 100 wt % elemental oxides for internal standardization of the LA-ICP-MS measurements.

attachment, an X'Celerator RTMS detector, and a Cu X-ray tube operated at 40 kV/40 mA (Ni filtered radiation). The beam path included a fixed 1/4° divergence slit, 1/2° antiscatter slits, and 0.02 rad soller slits. Five diffraction patterns were collected from 10° to 70° 2θ with a step size of 0.008° 2θ/step and a recording time of 50 s/step at 25, 50, 100, 150, and 200 °C.

Results

The microprobe results given in Table 2 represent the average composition obtained from a number of point analyses on four different crystals obtained from the first synthesis method. The individual analyses show small but measurable amounts of Al_2O_3 that is slightly variable and averaging roughly 1.3 wt %. It most likely originates from Al_2O_3 in the ceramic crucibles used for material preparation and synthesis, as the purity of the starting materials does not allow for it. We think the use of Li_2CO_3 or LiOH results in the production of a minor melt phase that dissolves Al_2O_3 from the crucible during sintering. Backscattered X-ray pictures revealed very small amounts, at roughly the 1−2% percent level, of $LaAlO_3$ and smaller amounts of what appears to be a La_3AlO_6 composition phase. Both occur as very tiny grains between garnet crystals. Other phases such as $LiAlO_2$ or Al_2O_3 could not be identified.

The LA-ICP-MS results on this same material are also given in Table 2. The data show excellent external reproducibility, 0.4% (1 SD) for La and 1.1% for Zr. Lithium and notably Al contents show, in comparison, some scatter of 3.5 and 20%, respectively. This is higher than the analytical uncertainty, demonstrating inhomogeneous distribution of these elements. Close inspection of transient signals revealed that Al signals increased when the laser beam drilled into holes or edges in the garnet grains, demonstrating that some Al could be located on surfaces. Consequently, the LA-ICP-MS analyses always included a subordinate fraction of surface related Al (i.e., that not visible in transient signal display). We interpret the LA-ICP-MS measurements as indicating an Al_2O_3 content in the garnet of about 1.1 wt %. There is also a slight correlation between decreasing Li contents with increasing La. No such relationship is observed between either Li or La with Zr.

Table 3. Structural Parameters at Room Temperature for Cubic Al-Containing $Li_7La_3Zr_2O_{12}$

atom	x	y	z	$U_{eq}/U_{iso(Li)}$ (Å^2)	occupancy
La	0.0	0.250	0.125	0.01048(6)	1.0
Zr	0.0	0.0	0.0	0.00807(7)	1.0
O	−0.03170(12)	0.05458(12)	0.14968(12)	0.0129(2)	1.0
Li1	−0.125	0.0	0.250	0.011(3)	0.37[a]
Li2	−0.0756(12)	−0.0971(12)	0.1880(12)	0.017(4)	0.28(2)

[a] Fixed to the value obtained from a refinement of the same crystal at 100 K.

Table 4. Selected Interatomic Distances (Å) in Cubic Al-Containing $Li_7La_3Zr_2O_{12}$

La−O × 4	2.5159(16)
La−O × 4	2.5886(16)
Zr−O × 6	2.1077(15)
Li1−O × 4	1.9135(16)
Li2−O	2.108(17)
Li2−O	1.854(16)
Li2−O	2.157(16)
Li2−O	2.250(16)
Li2−O	2.645(16)
Li1−Li2	1.626(15)
Li2−Li2	0.77(3)

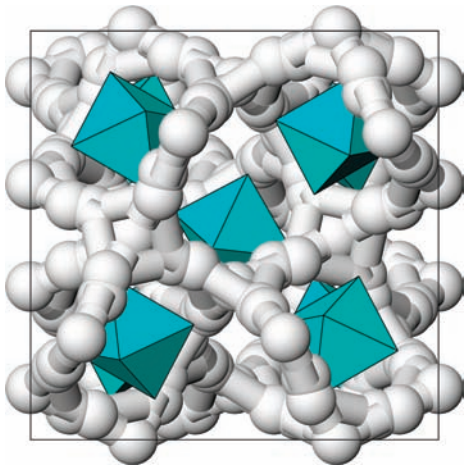

Figure 2. Crystal structure model for cubic Al-containing $Li_7La_3Zr_2O_{12}$ space group $Ia\bar{3}d$ projected on (100). Li sites are shown as white spheres, ZrO_6 octahedra are blue, and La atoms have been omitted for clarity. Adjacent Li positions are connected via white pathways that represent possible routes for Li diffusion.

The nature of the X-ray reflections indicates excellent crystallinity for the studied single crystal, and the final R factors indicate a very good refinement model. Atomic coordinates, adps, and site occupancy values are summarized in Table 3. Table 4 lists various bond lengths. Site population refinements indicate a La/Zr ratio of 3:2 and 4.5(2) Li atoms per-formula-unit could be located at two structural sites. The structure has space group $Ia\bar{3}d$ (Figure 2). The garnet octahedral B site (see discussion below for garnet crystal

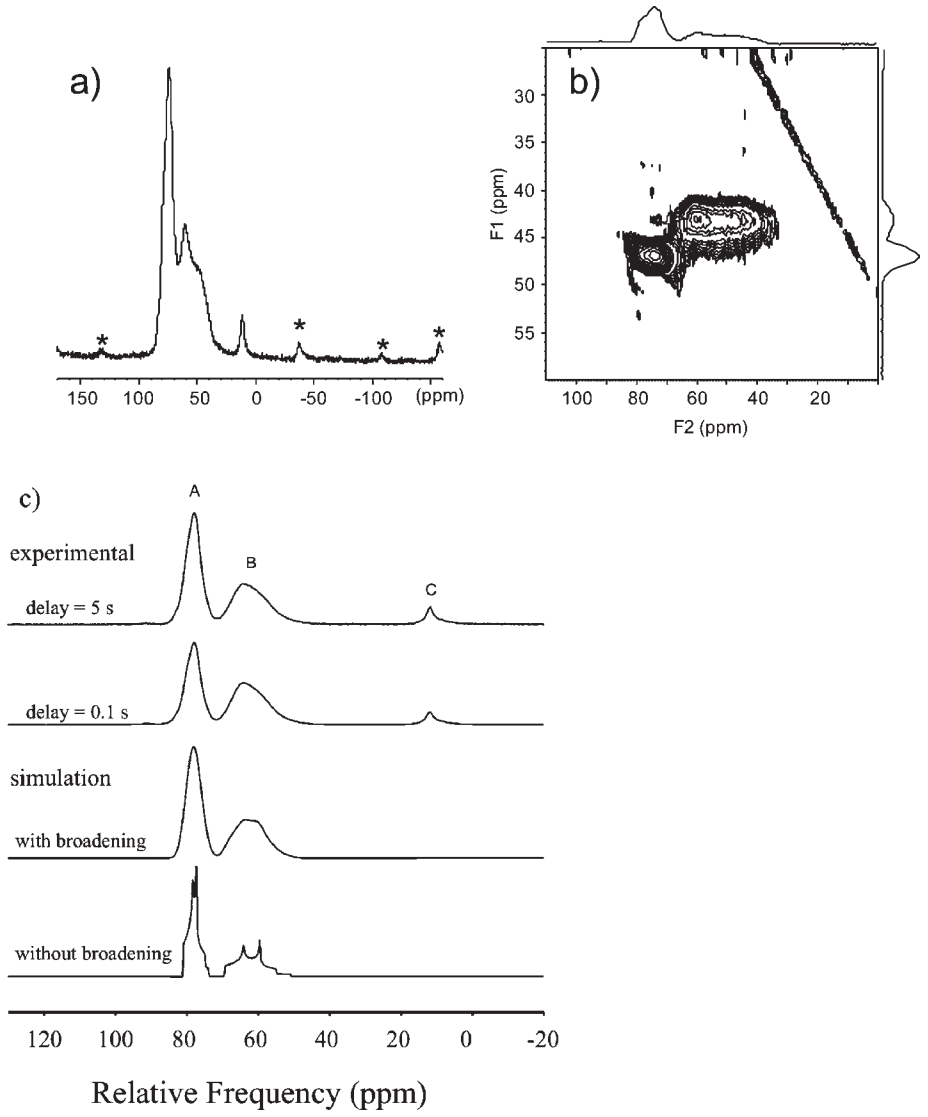

Figure 3. (a) Experimental ^{27}Al MAS NMR spectrum (Bochum) of cubic Al-containing $Li_7La_3Zr_2O_{12}$ showing two main resonances centered at about 80 and 68 ppm and spinning sidebands marked by asterisks. (b) ^{27}Al MQMAS spectrum (Bochum) with the isotropic F1 direction on the vertical axis and the F2 direction (corresponding to the one-dimensional experiment) on the horizontal axis. (c) Experimental ^{27}Al MAS NMR spectra (Stanford) of cubic Al-containing $Li_7La_3Zr_2O_{12}$ at 156.26 MHz with pulse delays of 0.1 and 5 s showing two main resonances centered at abut 81 and 70 ppm and simulated spectra with and without line broadening.

chemistry) is occupied by Zr and the 8-fold coordinated dodecahedral A site by La. Statistically, Li occupies about 1/3 of the tetrahedral C site, making this site roughly 2/3 vacant. Li is also located on a general crystallographic site (Table 3) approximately 1.6 Å from the C site, and it also shows a low occupancy of 0.28(2). It is bonded to five oxygens with Li−O bond lengths ranging from 1.85 to 2.65 Å.

In the ^{27}Al MAS NMR spectra (Figure 3a,c), three signals can be identified. Assignments are based on the crystal chemical behavior of Al in various oxides and silicates.[28] The signal at 11.8 ppm shows little intensity, is typical for octahedral Al, and is assigned to $LaAlO_3$ (Stebbins, personal communication). Two more intense signals occur at approximately 81 and 68 ppm.

Because of the strong line overlap in this spectral region that arises at lower magnetic fields, MQMAS NMR spectroscopy was performed to separate signals by their different isotropic chemical and quadrupolar shifts. The resulting two-dimensional ^{27}Al MQMAS NMR spectrum is shown in Figure 3b. Here, the two main Al signals can be distinguished. The isotropic shifts on the F1-frequency scale can be calculated for different field strengths according to the following equation:[29]

$$\Omega^{iso} = -\frac{17}{31}\Delta\sigma - \frac{8\times10^6}{93}\frac{\omega_Q^2}{\omega_0^2}\left(\frac{\eta^2}{3}+1\right) \qquad (1)$$

where $\Delta\sigma$ is the difference between the isotropic chemical shift and the reference, $\omega_Q = 6C_Q/2I(2I-1)$, ω_0 is the Zeeman frequency, and C_Q and η are the quadrupolar parameters. 2D spectra were sheared using a t_1-dependent phase increment following the Fourier transformation in the directly detected dimension (F2). Both the isotropic F1 axis and the position of

(28) Stebbins, J. F. In *Mineral Physics and Crystallography: A Handbook of Physical Constants*; Ahrens, T.J., Ed.; American Geophysical Union: Washington, DC, 1995; pp 303−332.

(29) Massiot, D.; Touzo, B.; Trumeau, D.; Coutures, J. P.; Virlet, J.; Florian, P.; Grandinetti, P. J. *Solid State Nucl. Magn. Reson.* **1996**, *6*, 73–83.

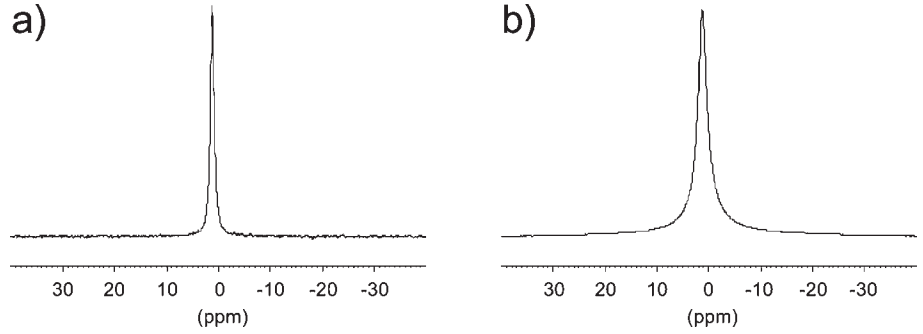

Figure 4. (a) ^{6}Li NMR MAS spectrum of cubic Al-containing $Li_7La_3Zr_2O_{12}$. The line has a fwhm of 0.8 ppm. (b) ^{7}Li NMR MAS spectrum of $Li_7La_3Zr_2O_{12}$. The line has a fwhm of 2.2 ppm. The chemical shift values for both are 1.2−1.3 ppm.

0 ppm with respect to the transmitter frequency were scaled by a factor of 12/31.[29] The ^{27}Al MAS NMR spectrum was fitted with quadrupolar MAS line shapes including Lorentzian convolution using the DmFit 2009 program.[30]

Because of the low signal intensity associated with octahedral Al in $LaAlO_3$, it cannot be observed in the MQMAS NMR spectrum. The signal at δ(F2) = 81 ppm and δ(F1) = 47 ppm exhibits a quadrupolar pattern with a quadrupolar coupling constant C_Q = 3.3 MHz and an asymmetry parameter η = 0.7, indicating an asymmetric coordination geometry. The second signal at δ(F2) = 68 ppm and δ(F1) = 43 ppm shows stronger quadrupolar interaction and has C_Q = 5.0−5.2 MHz and a much lower value of η = 0.0−0.1 indicating axial symmetry. However, it is difficult to fit this signal precisely, because a possible third overlapping signal could be present.

The ^{27}Al MAS NMR spectra recorded at 156.26 MHz show features similar to those at 104.27 MHz but with better resolution of the two resonances at high frequency. They are labeled A and B in Figure 3c. Once again, the position and shape of peak C is consistent with the presence of minor $LaAlO_3$. Two spectra were collected with interpulse delays of 0.1 and 5 s. Peak B appears to be fully relaxed with the 0.1 s delay, while peaks A and C have somewhat longer relaxation times. The relative ratio between the resonances A/B is approximately 6:4. The experimental resolution at this magnetic field makes it possible to simulate their line shapes, yielding an isotropic chemical shift of 81 ppm with C_Q of 3.3 MHz and η of 0.7 for peak A and 70 ppm, 5.5 MHz and 0.5 for peak B. The chemical shift values for peak A agree well with those obtained from the MQMAS. However, the simulation for peak B is not perfect and the derived NMR parameters are slightly different from those of the MQMAS. It is possible that more than one Al site is represented by peak B, as discussed above for the MQMAS data.

Assignments for these two main ^{27}Al resonances are not a simple matter. Solely on the basis of their chemical shift values, both should correspond to Al in 4-fold coordination. The X-ray results show, however, only a single tetrahedral coordination polyhedron. The resonance located at 68 ppm could correspond to Al at the tetrahedral Li site based on its chemical shift value and its low asymmetry parameter of approximately zero. The assignment of the other peak at 80 ppm is difficult. The chemical shift clearly indicates 4-fold coordination. Because of the low Al-content of the garnet, aluminum cannot be detected by the X-ray diffraction experiment. It is proposed that this Al occupies the Li2 site, which is a distorted site with approximate 5-fold coordination as given by the diffraction experiment and which has an asymmetric NMR parameter. It is possible that Al adopts a different coordination geometry locally than Li at Li2.

Both ^{7}Li and ^{6}Li MAS NMR spectra exhibit one narrow resonance at 1.2−1.3 ppm (Figure 4). Crystallographically different coordinated Li atoms cannot be distinguished in the NMR experiment in the case of cubic Al-containing $Li_7La_3Zr_2O_{12}$ at room temperature. ^{7}Li NMR resonances are affected by homonuclear dipolar and second-order quadrupolar interactions. Both interactions lead to an increased line width. The smaller quadrupolar and homonuclear dipolar broadening for ^{6}Li gives rise to the narrower resonance.

Powder diffraction results obtained on $Li_7La_3Zr_2O_{12}$ garnet synthesized solely in the Pt crucible are shown in Figure 5. All peaks could be indexed to garnet. At room temperature, this phase is noncubic, but at higher temperatures changes in the diffraction pattern become apparent. Following the synthesis procedure in ref 20, a phase transition occurs from tetragonal ($I4_1/acd$) to cubic ($Ia3d$) symmetry between 100 and 150 °C. The phase transition is expressed, for example, in the merging of the (121) and (112) peaks at 16.63° 2θ and 16.94° 2θ, respectively, which are present at 25, 50, and 100 °C, into one (112) peak at 16.78° 2θ, which is present at 150 and 200 °C.

Discussion

Crystal Chemistry and Structural Properties of Li-Oxide Garnets and "$Li_7La_3Zr_2O_{12}$". The structural and crystal chemical properties of various oxide-based garnets, whose general formula can be given as $^{XII}A_3{}^{VI}B_2{}^{IV}C_3O_{12}$, have been investigated intensively by X-ray and neutron diffraction experiments since Menzer first solved the structure.[31] Most garnets, for example, the silicate,[32,33] the YIG/YAG,[34] and the Li-oxide types,[11−17,19,21−23] generally have the cubic space group $Ia\bar{3}d$. However, it should be stressed that this may not always be the case[9,10,18,20] (and see discussion below). This has led to considerable confusion in the literature with regard to the crystal chemical properties of the Li-oxide class of garnets.

(30) Massiot, D.; Fayon, F.; Capron, M.; King, I.; Le Calvé, S.; Alonso, B.; Durand, J. O.; Bujoli, B.; Gan, Z.; Hoatson, G. *Magn. Reson. Chem.* **2002**, *40*, 70–76.

(31) Menzer, G. *Zeit. Kristall.* **1928**, *69*, 300–396.

(32) Geiger, C. A. In *Spectroscopic Methods in Mineralogy, European Mineralogical Union Notes in Mineralogy*; Libowitzky, E., Beran, A., Eds.; European Mineralogical Union: Wien, Austria, 2004; Vol. *6*, pp 589−645.

(33) Geiger, C. A. *Am. Mineral.* **2008**, *93*, 360–372.

(34) Winkler, G. *Magnetic Garnets*; Friedr. Vieweg & Sohn Verlagsgesellschaft GmbH: Braunschweig, 1981.

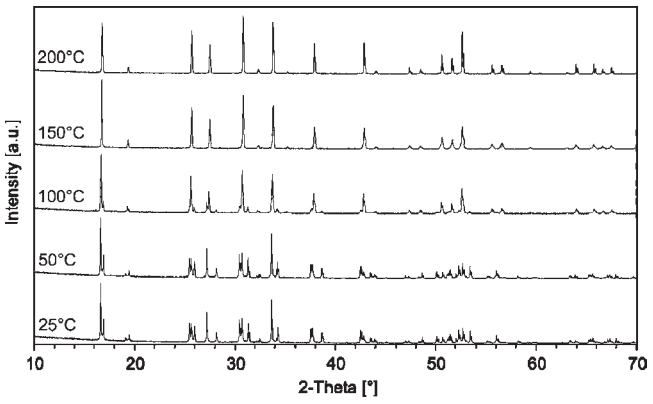

Figure 5. Powder X-ray patterns of pure $Li_7La_3Zr_2O_{12}$ as a function of temperature. All peaks could be indexed to garnet. A phase transition from tetragonal to cubic symmetry occurs between 100 and 150 °C.

In space group $Ia\bar{3}d$ the cations for $^{XII}A_3{}^{VI}B_2{}^{IV}C_3O_{12}$ stoichiometric-type garnets are located at special crystallographic positions and the oxygen atoms at a general position. Thus, the basic crystal structure can be described by knowledge of the unit-cell parameter *a* and the *x*, *y*, *z* atomic coordinates for oxygen. Various cations can occupy the A site (Wyckoff 24*c* position) of 222 point symmetry, the B site (16*a* position) of $\bar{3}$ symmetry and the C site (24*d* position) of $\bar{4}$ point symmetry. The structure consists of CO_4 tetrahedra and BO_6 octahedra that are connected over shared corners and cations that are coordinated by eight oxygen atoms that form a triangular dodecahedron AO_8. There are a large number of shared cation-coordination polyhedral edges in the structure.

All Li-oxide garnets are characterized by having Li in tetrahedral coordination (C site or 24*d*). The A and B positions can be occupied by a large variety of cations of different sizes and formal charges. There are Li-oxide garnets with "standard" garnet stoichiometry such as $Li^C{}_3Nd^A{}_3W^B{}_2O_{12}$, for example, and they are poor ion conductors.[13] However, because of the ability of the garnet structure to accept a large variety of atoms of different sizes and charges, a number of different Li-oxide garnets have been synthesized with Li at additional sites. These garnets can have nominally 4, 5, 6, or 7 Li cations and for solid solutions even noninteger values in the formula unit. Examples are $Li_4Nd_3TeSb_2O_{12}$, $Li_5Ln_3Sb_2O_{12}$ with Ln = La, Pr, Nd, Sm, and Eu, $Li_6ALa_2Nb_2O_{12}$ with A = Ca, Sr, and Ba, $Li_7La_3Sn_2/Zr_2O_{12}$, and $Li_{6.4}Sr_{1.4}La_{1.6}Sb_2O_{12}$.[19,7,17,2,18,5,16]

These compositions, as well as a number of others,[8] have been the focus of much recent work with regard to their fast Li-ion conductivity. The various garnets, with reported cubic and lower symmetries, show a range of behavior, and increased conductivity does not necessary increase with the amount of Li. In Li-oxide garnets with greater than three Li atoms in the formula unit, Li is located at additional structural positions.[11−23] The coordination polyhedron for one of these sites represents a very distorted octahedron. It shares faces with the LiO_4 tetrahedra, and because of the short Li−Li distances positional disorder can result, as first described in $Li_5La_3M_2O_{12}$ with M = Ta or Sb.[11] In this arrangement, the different Li sites are not fully occupied and clustering and/or different local environments are thought to occur. It has been proposed that they act to minimize cation−cation repulsion.[11]

A description of the precise crystal chemical properties of Li-oxide garnets is hampered by the difficulty in obtaining interpretable adps in the diffraction experiment. It is often the case that powder diffraction data sets, even using neutrons, are insufficient to address this problem. This issue is important because a quantitative determination of the adps is necessary to obtain correct Li-site occupancies. Site occupancies and thermal motion for a given atom are correlated in the refinement procedure.[35] Thus, we think that most (all?) X-ray powder diffraction data sets collected on Li-oxide garnets are of insufficient quality to describe the adps and site occupancy for the Li sites correctly. It is notable, furthermore, that in some neutron powder diffraction studies[11,14,15] the reported adps for Li are difficult to understand from a crystal chemical standpoint. For example, reported adps for Li at C (24*d*) are larger than those for Li at the B (48*g*) and their general 96*h* site[11,14] or they show large experimental uncertainties.[15] It is expected that Li at the tetrahedral C-site, where Li is relatively strongly bonded, should have smaller adps than Li at higher coordination sites or in irregular coordination geometries. On the basis of our investigations on silicate garnets (see review of the various studies in ref 33), we think that only large diffraction data sets collected up to high two-theta values on single crystals can begin to address the issue of adps and site occupancies.

The present X-ray single-crystal results on cubic Al-containing $Li_7La_3Zr_2O_{12}$, based on about 16 000 total reflections and 770 unique reflections, are generally consistent with the more recent published crystal chemical properties of other Li-oxide garnets. However, our results do show some differences. This mainly involves the nature of the Li cations. Two crystallographic Li sites could be determined in this work (Figure 2; Table 3). The X-ray refinements can possibly be interpreted as indicating a third Li site of low occupancy whose position is analogous to that described in $Li_5La_3M_2O_{12}$ (M = Ta, Nb),[11] but a confirmation of this is not possible at this time. We chose, here, not to over interpret the X-ray data. The precise positions of the remaining Li atoms could not be determined, and they are assumed to be structurally delocalized. This behavior has been noted in fast-ion conductors using diffraction methods, where it is often difficult to distinguish between regular crystallographic and interstitial sites.[36]

The refined adp values for the various atoms in cubic Al-containing $Li_7La_3Zr_2O_{12}$ garnet appear reasonable and well behaved as a function of temperature. Figure 6a shows the U_{eq} values determined from refinements made from 100 to 500 K for La, Zr, and O. They show a typical increase with increasing temperature, and the largest values are associated with the oxygen atoms. Figure 6b shows a similar plot for the two crystallographically different Li atoms. The refined U_{eq}/U_{iso} values of 0.011 and 0.017 Å^2 for Li1 (24*d*) and Li2 (96*h*) at 300 K, for example, are reasonable crystal chemically.

Crystal Chemistry and Conductivity Behavior of Li-Oxide Garnets and "$Li_7La_3Zr_2O_{12}$". There has been much discussion on the conductivity mechanism(s) for the various Li-oxide garnets based on their crystal-chemical properties,

(35) Yamazaki, S.; Toraya, H. *J. Appl. Crystallogr.* **1999**, *32*, 51–59.
(36) Schulz, H. *Ann. Rev. Mater.* **1982**, *12*, 351–376.

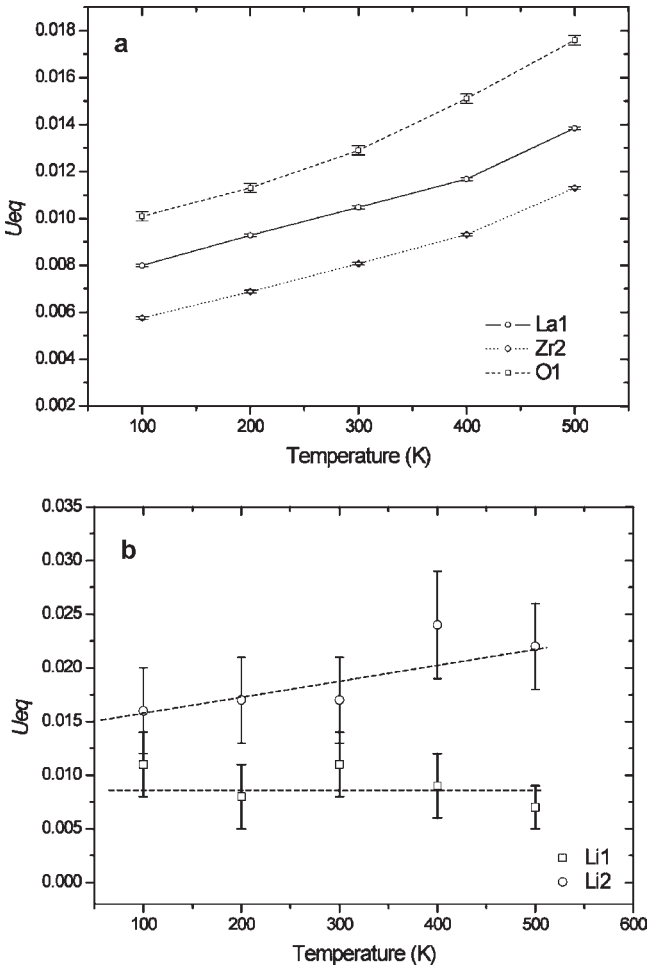

Figure 6. (a) Variation in the diffraction U_{eq} values for the atoms O, La, and Zr from 100 to 500 K in cubic Al-containing $Li_7La_3Zr_2O_{12}$. (b) Variation in the diffraction U_{eq} values for Li1 (C tetrahedral site) and Li2 (5-fold coordinated site) from 100 to 500 K.

Li NMR spectra, and bond-valence calculations.[6,19,37−39] There is little agreement between the various investigations, and it is possible that different mechanisms exist for the various garnet phases. It is of critical importance for such analysis that the crystal chemical model is correct and that the Li-atom behavior is described properly. An understanding of the crystal chemical and structural properties of the two structural modifications of "$Li_7La_3Zr_2O_{12}$" is useful for understanding the possible nature of ion conductivity for Li-oxide garnets in general.

Tetragonal $Li_7La_3Zr_2O_{12}$ shows slightly lower ion conductivity,[20] about 1 order of magnitude less at ambient conditions (Figure 1), than cubic "$Li_7La_3Zr_2O_{12}$" as given in ref 5, whose precise composition was not determined. An X-ray single-crystal refinement made on flux-grown tetragonal $Li_7La_3Zr_2O_{12}$ at room temperature, with atomic ratios Li/La/Zr = 7.0:3.0:1.9 as determined by ICP-OES measurements and free of other elements, gave space group $I4_1/acd$.[20] Here, the Li cations are ordered and they occur on three different crystallographic sites, namely, 8*a*, 16*f*, and 32*g*. Notably, moreover, vacant tetrahedral sites (16*e*) are present. The structure is shown in Figure 7a,b. The crystal structure of tetragonal $Li_7La_3Sn_2O_{12}$,[18] which also conducts less well than cubic "$Li_7La_3Zr_2O_{12}$", is similar to that of tetragonal $Li_7La_3Zr_2O_{12}$. In tetragonal $Li_7La_3Zr_2O_{12}$ and $Li_7La_3Sn_2O_{12}$, the potential diffusion pathways are anisotropic in nature being different in the (001) and (100) planes.

The cubic Al-containing $Li_7La_3Zr_2O_{12}$ $Ia\bar{3}d$ structure studied here represents a disordered modification of the tetragonal phase described in ref 20. In the cubic phase, several properties could lead to the high Li conductivity. They are: (i) the single crystallographic tetrahedral C site (24*d*) that is statistically occupied with roughly 1/3 Li atoms; (ii) the short distances between the Li sites; (iii) the adps for all atoms that are approximately a factor of 2 larger than the corresponding ones for the tetragonal phase. Moreover, the U_{eq} values remain large even at 100 K. This indicates greater static disorder of the Li atoms in cubic $Li_7La_3Zr_2O_{12}$ compared to tetragonal $Li_7La_3Zr_2O_{12}$, and (iv) The diffusion pathways are isotropic in the Al-containing cubic phase. The $I4_1/acd$ tetragonal modification has anisotropic pathways resulting from Li ordering.

In terms of dynamics, the ^{6}Li and ^{7}Li NMR results on cubic Al-containing $Li_7La_3Zr_2O_{12}$ show single resonances with narrow line widths (Figure 4). This reflects fast-ion diffusion at room temperature. The Li ions experience a time-averaged oxygen coordination and chemical shift interaction similar to Li ions in aqueous solution. Additional evidence for the fast diffusion is the very short spin−lattice relaxation time for the ^{6}Li isotope, which is normally long. Li chemical shift values in oxides and silicates range from about +1.5 ppm for the LiO_3 site in Li_4SiO_4 to around +1 to 0 ppm for Li at tetrahedral sites to about −1.0 ppm for Li atoms in octahedral coordination.[40] Thus, the observed chemical shifts for Li of 1.2−1.3 ppm in Al-containing cubic $Li_7La_3Zr_2O_{12}$ garnet suggest that the Li atoms are spending most of their time at the tetrahedral C (24*d*) site. This interpretation agrees with the diffraction adp values obtained for Li, because they are smallest for the tetrahedral C site.

The Li-oxide garnet phase $Li_5La_3Nb_2O_{12}$ has received the most extensive Li NMR study.[37,38] ^{6}Li-MAS NMR spectra showed two lines at about −0.2 ppm and 0.7 ppm for a sample annealed at 850 °C and −0.6 ppm and 0.4 ppm for a sample annealed at 900 °C.[37] The relative intensities of the two lines are dependent on the annealing temperature of the sample and the resonances were assigned to Li at tetrahedral and octahedral sites. The results were interpreted as indicating that the Li atoms in tetrahedral coordination are immobile, whereas those at the octahedral site contribute to the dynamics of the system.[37] ^{7}Li-MAS NMR spectra, made as a function of temperature, showed a single resonance that was fit using two superposed lines.[38] $Li_5La_3Nb_2O_{12}$ is characterized by lower Li conductivity than $Li_7La_3Zr_2O_{12}$.

(37) van Wüllen, L.; Echelmeyer, T.; Meyer, H.-W.; Wilmer, D. *Phys. Chem. Chem. Phys.* **2007**, *9*, 3298–3303.
(38) Koch, B.; Vogel, M. *Solid State Nucl. Magn. Reson.* **2008**, *34*, 37–43.
(39) Thangadurai, V.; Adams, S.; Weppner., W. *Chem. Mater.* **2004**, *16*, 2998–3006.
(40) Xu, Z.; Stebbins, J. F. *Solid State Nucl. Magn. Reson.* **1995**, *5*, 103–112.

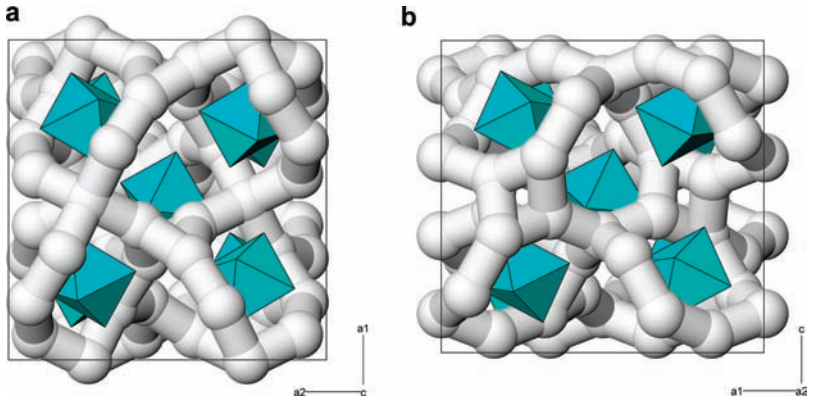

Figure 7. (a, b) Crystal structure model for tetragonal $Li_7La_3Zr_2O_{12}$ (ref 20) projected on (001) and (100), respectively. Note that possible Li diffusion pathways are different for the two orientations.

A valence bond analysis on $Li_5La_3M_2O_{12}$ with M = Nb and Ta was made to determine the nature of the Li-conduction process in the garnet. This was done under the assumption $I2_13$ and $Ia\bar{3}$ symmetries.[39] This gives Li-site distributions in the garnet structure that are questionable based on the present X-ray data and recent published neutron diffraction results that give space group $Ia\bar{3}d$.

It is proposed, based on the results of this study on cubic Al-containing $Li_7La_3Zr_2O_{12}$, that all the Li atoms are involved in the conduction process. This is consistent with the static crystal chemical model and the possible diffusion pathways as given by the diffraction experiment and also the Li NMR results (Figure 2). Li NMR measurements made over a range of temperatures could give further insight into the diffusion behavior of Li in "$Li_7La_3Zr_2O_{12}$".

Phase Stability of "$Li_7La_3Zr_2O_{12}$" Garnet with and without Al and Conductivity Behavior. "$Li_7La_3Zr_2O_{12}$" garnet shows some of the highest ion-conductivity behavior yet reported for a crystalline phase (Figure 1). This Li-oxide garnet was first described in ref 5 and was also synthesized in Al-containing ceramic crucibles, but was not characterized compositionally. Therefore, its exact composition is uncertain and it could have contained Al. Recent conductivity measurements on a series of cubic Al-containing $Li_7La_3Zr_2O_{12}$ garnets (Weppner, unpublished) show ion conductivity behavior similar to that reported in ref 5. One issue to be addressed in future work is the possible presence of compositional zoning or of another phase occurring on garnet grain boundaries. If either occurs, conductivity behavior could be affected.

Phase stability for Al-free $Li_7La_3Zr_2O_{12}$ garnet would appear to be analogous to that of $Li_7La_3Sn_2O_{12}$ garnet.[15] In both, the tetragonal modification is stable at lower temperatures, whereas the cubic phase is the nonquenchable high-temperature form. This begs the question, again, of why the garnet studied in ref 5 is cubic. Either this phase contained some undetected Al or it has some other crystal chemical difference that differentiates it from the tetragonal phase that should be stable at ambient conditions. We think the former is more probable. We note, however, that the issue of the precise Li concentrations in Li-oxide garnets and their exact stoichiometric formulas is also a difficult issue that has not been addressed in a careful manner. Because of the synthesis methods employed, which normally start with an overabundance of a Li-containing starting material and that use different sintering temperatures and times, it is possible that the Li contents may vary from the nominal formulas that are normally assumed. There may be small differences in composition and also structure. More research is needed to address this issue. In addition, the effect of small concentrations of dopants (here Al) that may stabilize the cubic phase needs to be studied.

We propose a simple crystal chemical model to explain why cubic Al-containing $Li_7La_3Zr_2O_{12}$ is (meta)stable at ambient conditions and why it is such a good ion conductor. First, a heterovalent substitution mechanism(s) of the type $Al^{3+} \Leftrightarrow 3Li^+$ may act to stabilize the cubic phase relative to the tetragonal structure. The substitution of small amounts of an atom in a substitutional solid solution can stabilize a given structure in pressure−temperature−compositional space,[41] and Al may act to do this in $Li_7La_3Zr_2O_{12}$ garnet. Second, this substitutional mechanism may act to decrease the Li site occupancies. Increased numbers of empty structural sites could permit increased Li^+ ion mobility and thus conductivity. In terms of phase relations, tetragonal $Li_7La_3Zr_2O_{12}$ is the thermodynamically stable phase in the pure three-component system $Li_2O-La_2O_3-ZrO_2$ at ambient conditions. However, further work is required to determine the exact phase relations as a function of temperature, as well as the effect of heterovalent substitution mechanisms on garnet stability and ion-conductivity behavior.

Acknowledgment. We thank J. F. Stebbins (Stanford University) and R. Murugan for helpful discussions. The critical comments of two reviewers led to a revision that helped clarify several aspects of this study.

(41) Armbruster, T.; Basler, R.; Mikhail, P.; Hulliger, J. *J. Solid State Chem.* **1999**, *145*, 309–316.